Performance of ultrasonic speckle tracking in various tissues[a)]

Eric J. Chen, W. Kenneth Jenkins, and William D. O'Brien, Jr.
Department of Electrical and Computer Engineering, 1406 W. Green Street, University of Illinois, Urbana, Illinois 61801

(Received 6 April 1994; accepted for publication 4 April 1995)

The purpose of this study was to investigate the accuracy of ultrasound speckle tracking in various tissues. Results from two-dimensional tissue speckle tracking in liver, muscle, fat, and sponge samples are presented, while keeping other speckle tracking parameters constant. Speckle tracking performance was characterized both in terms of the magnitude of tracking errors and in terms of the percentage of correctly tracked displacement vectors. Speckle tracking in muscle tissue, which contains myofibrils and significant tissue microstructure, produced the highest percentage of correctly tracked vectors and smallest tracking errors relative to other tissues. © *1995 Acoustical Society of America.*

PACS numbers: 43.80.Ev, 43.80.Jz, 43.80.Vj

INTRODUCTION

The goal of this work is to investigate the accuracy of ultrasound speckle tracking in various tissues. Speckle tracking has been widely used in ultrasonic blood velocity measurements (Chen *et al.*, 1989), in noninvasive ultrasonic elasticity imaging of hard tumors (O'Donnell *et al.*, 1994), in intravascular imaging of arterial walls (Ryan *et al.*, 1993), and in phase aberration correction techniques (O'Donnell and Engeler, 1992). The reliability of ultrasonic blood velocity, tissue elasticity, and phase aberration correction measurements all depend on the accurate performance of speckle tracking.

Elasticity imaging, for example, often requires two-dimensional speckle tracking of small areas of tissue to estimate internal tissue displacement. Tissue displacements are then used to reconstruct tissue strain fields. Errors in speckle tracking resulting in errors in displacement estimates directly influence the accuracy of strain estimates and ultimately reconstructed elasticity fields. In a similar fashion, measurements of phase aberrations and blood velocity depend on reliable speckle tracking. Thus it is critical to understand to what degree speckle tracking measurements are reliable and how different factors may affect the reliability of those results. Of particular interest is the effect of various tissues on speckle tracking. In this study, we investigate the performance of speckle tracking in liver, muscle, and fat tissues, while keeping other speckle tracking parameters such as ultrasound frequency and region of interest (ROI) dimensions constant. The effects of other important imaging parameters on speckle tracking accuracy have been reviewed by Chen *et al.* (1994).

I. TWO-DIMENSIONAL SPECKLE TRACKING

Two-dimensional speckle tracking algorithms estimate tissue motion by comparing speckle patterns in serially acquired ultrasonic images. The speckle patterns are used as landmarks or registration points to determine relative motion. To estimate local tissue displacement, a window of data corresponding to the tissue ROI is selected from an initial ultrasound scan. This window of data is compared with identically sized windows of data (templates) inside of a predefined search region in a successive ultrasound scan until a best match is found. The position of the window in the initial scan and the position of the best match window in the successive scan are used to determine the net displacement of the tissue region between scans. A two-dimensional displacement vector is computed for each ROI. Displacement vectors are assumed to start in the center of ROIs and all pixels in the ROI are assumed to translate by the magnitude and direction of the displacement vector. In this manner velocity of tissue motion can also be determined if the elapsed time between scans is known. A statistical correlation coefficient is used to determine the best match.

If x and y represent two variables or windows of data, then a normalized correlation between the two variables can be computed according to (Chen *et al.*, 1989, 1991)

$$\rho_{xy}=\frac{\mathrm{Cov}(x,y)}{\sqrt{\mathrm{Var}(x)\,\mathrm{Var}(y)}}, \tag{1}$$

where the covariance and variance functions are defined as

$$\mathrm{Cov}(x,y)=E[(x-\bar{x})(y-\bar{y})] \tag{2}$$

and

$$\mathrm{Var}(x)=E[(x-\bar{x})^2] \tag{3}$$

and x, y and $\bar{x}$, $\bar{y}$ are two variables and their mean values, respectively. If x, y are two different images, then the discrete version of the correlation coefficient shown in Eq. (2) can be used (Chen *et al.*, 1991):

$$\rho_{xy}(k,l)=\frac{\sum_{i=1}^{M}\sum_{j=1}^{N}(x(i,j)-\bar{x})(y(i+k,j+l)-\bar{y})}{\sqrt{\sum_{i=1}^{M}\sum_{j=1}^{N}(x(i,j)-\bar{x})^2\sum_{i=1}^{M}\sum_{j=1}^{N}(y(i+k,j+l)-\bar{y})^2}}, \tag{4}$$

[a)]This work was supported by the National Institutes of Health Grant No. 5 T32 CA 09067.

 0001-4966/95/98(3)/1273/6/$6.00

where $x(i,j)$, $y(i,j)$ represent two $M \times N$ windows of data in the ultrasound images x, y, the variables (k,l) represent the pixel coordinates of the template region in the second image, and $\bar{x}$, $\bar{y}$ are the mean pixel values in the windows $x(i,j)$, $y(i,j)$.

II. METHODS

Four types of samples, three tissues and one sponge, were used in speckle tracking experiments. Tissue samples consisted of porcine muscle, liver, and fat obtained from the Meat Sciences Laboratory, Department of Animal Sciences at the University of Illinois. Tissue samples were approximately 150 mm in length and 100 mm by 100 mm in width and height and were vacuum sealed. Tissue samples were packed in ice and transported to the Bioacoustics Laboratory for experiments within 24 h of death. The sponge sample consisted of a standard commercially available fine pore urethane sponge with dimensions of 150 mm×100 mm×100 mm. Similar sponge targets have been used in previous studies (Trahey *et al.*, 1986) and have been shown to produce reasonable speckle images. A histogram of pixel intensities was also used to verify speckle scattering. Samples were placed below an ATL transducer and secured on top of sound absorbing slabs near the bottom of a water tank. Ultrasound B-scan images of samples were acquired using a 5.0-MHz, 742A ATL servo-controlled rotary system coupled to an ATL MK-500 imaging system. The ATL transducer had a 9.5-mm-diameter crystal and used a mechanical sector scan with a 4.0-cm focal distance, and with a focal region extending from 2.0 to 6.0 cm. Samples were positioned in the approximate center of the transducer's focal region and were imaged in a manner to cover the entire field of view of ultrasound B scans. All measurements were performed at room temperature (22 °C) and the position of all tissue samples remained fixed throughout the experiment.

To simulate axial and lateral tissue motion, the transducer was translated using a high-precision Daedal motorized positioning system (precision of 5 μm for axial and lateral motion). The positioning system is computer controlled and has five degrees of freedom, three translational and two rotational. Sequentially acquired frames of tissue motion were digitized using a Targa-16 frame grabbing system with a spatial sampling of approximately 0.25 mm per pixel in both the axial and lateral directions. Digitized gray scale images were ported to a Sun Sparc 20 workstation for speckle tracking and analysis. A sequence of ten images was acquired for each tissue. The following speckle tracking parameters were held constant throughout the experiment: ultrasound frequency (5 MHz), magnitude and direction of motion (axial and lateral translations in 1.0-mm increments), and ROI size (3.0 mm×8.0 mm).

To characterize the performance of speckle tracking in each of the tissues, displacement vectors were computed for ROIs inside of the focal region and speckle tracking performance was calculated in terms of the percentage of correctly tracked displacement vectors. The size of the search region used in both the axial and lateral directions was 1.3× the magnitude of the actual displacement. Similarly sized search regions were used in previous studies and shown to provide reasonable speckle tracking (Ramamurthy and Trahey, 1991). Following the convention of previous groups (Trahey *et al.*, 1988), displacement vectors tracked within 30% of the actual displacement in the axial and lateral directions were considered correct. Thirty-two displacement vectors were calculated for each translation. The dimension of ROIs was 3.0 mm×8.0 mm or approximately four resolution lengths in each dimension (Wagner *et al.*, 1985).

An incremental tracking algorithm was used to measure large displacements. Using this algorithm, large displacements were obtained by summing smaller interframe displacements. For example, a 3.0-mm displacement between frames 1 and 4 in an image sequence is estimated by summing the differential displacements between frames 1-2, 2-3, and 3-4.

The magnitude of tracking errors was computed for all ROIs tracked in all tissues. Tracking error was defined as the geometric distance between actual and tracked displacements and is mathematically defined as

$$e = \sqrt{((x_t - x_o)^2 + (y_t - y_o)^2)}, \tag{5}$$

where (x_o, y_o) and (x_t, y_t) denote the actual and tracked coordinates of displacement, respectively.

Tissue autocovariance curves were generated by selecting an axial or lateral line of data passing through the center of digitized images of each tissue type. An autocovariance sequence was computed for each line of data using the sample autocovariance estimator

$$C(k) = \sum_{i=0}^{N-|k|-1} (x(i) - \bar{x})(x(i+k) - \bar{x}) \tag{6}$$

and normalized to amplitude values between 1.0 and −1.0.

III. RESULTS

Quantitative comparison of speckle tracking performance in each of the tissues in terms of percentage of correctly tracked vectors is shown in Fig. 1. Axial speckle tracking accuracy was approximately the same in all tissues. Almost all ROIs were correctly tracked in all of the tissues for displacements up to 3.0 mm. In the lateral direction, for displacements up to 2.0 mm, speckle tracking performance was comparable in all tissues. For larger displacements (2.0–4.0 mm), speckle tracking accuracy in liver was approximately 10% lower than in the control sponge, and approximately 20% lower than in muscle. Speckle tracking performance can also be plotted as a function of the imaging system axial and lateral resolution. Axial speckle tracking results are shown over a slightly smaller displacement range so that the maximum translation in both directions is equivalent to approximately four resolution lengths.

Tissue speckle tracking errors for axial and lateral translations are shown in Fig. 2. Tracking errors shown are the average of tracking errors from speckle tracking ten separate, nonoverlapping ROIs. Tracking errors appeared to be consistently lower in muscle tissue relative to the control sponge, and consistently higher in fat for both axial and lateral translations.

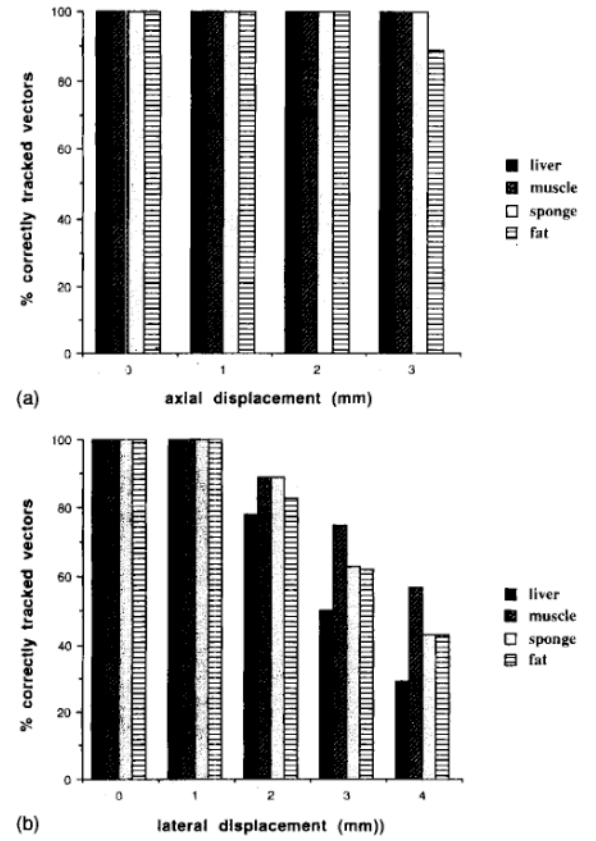

FIG. 1. Tissue speckle tracking performance quantified in terms of the percentage of correctly tracked vectors [see Eq. (5); based on 30% criterion] for (a) axial translations and (b) lateral translations. Thirty-two displacement vectors were tracked for each translation.

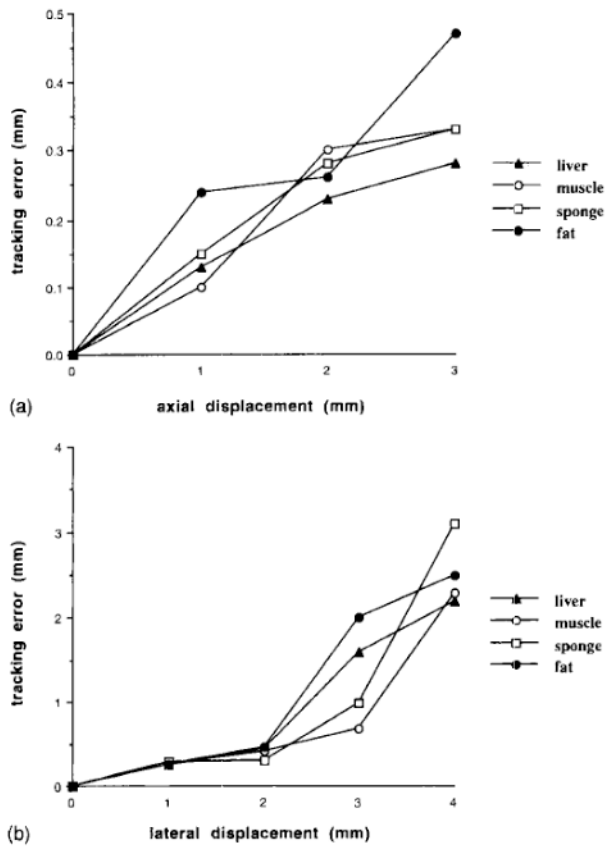

FIG. 2. Tissue speckle tracking performance quantified in terms of magnitude of tracking errors for (a) axial translations and (b) lateral translations. Tissue tracking errors were averaged from ten independent, nonoverlapping ROIs.

The axial and lateral experimental autocovariance curves for liver, muscle fat, and control sponge are shown in Fig. 3. Measurements were averaged over five axial and lateral lines of data.

Speckle pattern decorrelation for axial and lateral translations of the control sponge are shown in Fig. 4. Data points are the average of five independent, nonoverlapping ROIs.

IV. DISCUSSION

The performance of speckle tracking depends on a number of ultrasonic imaging parameters including magnitude and direction of tissue motion, ROI dimensions, ultrasonic frequency, and tissue type. The two-dimensional performance of tissue speckle tracking was quantified in terms of the percentage of correctly tracked displacement vectors in three different tissue types, while keeping other parameters constant.

All measurements in tissues were compared with measurements of a control sponge. Similar sponge targets have been used by previous groups and have been shown to generate reasonable ultrasound speckle images (Trahey *et al.*, 1986).

Because ultrasonic echoes result from internal tissue variations of acoustic parameters, differences in the variation of propagation speed inside of each tissue type may result in different signal-to-noise ratios in the echoes received from each tissue. In addition, attenuation effects could result in a downshift in the center frequency of reflected echoes, thus changing the effective ultrasonic frequency of interrogation and affecting tracking accuracy. The propagation speeds for all four sample types are within 5% of one another (Goss *et al.*, 1978). Also, the differences in attenuation between liver and muscle are typically less than 10% (Goss *et al.*, 1980) and downshifts in frequency due to attenuation are typically on the order of only a few hundred kilohertz for a center frequency of 5.0 MHz. Thus the relative contribution from these effects should remain relatively small.

Speckle tracking performance will also be clearly dependent on the transducer axial and lateral resolution and focusing characteristics. Since B-mode images were acquired using a mechanical scan transducer with a fixed focal distance, all ROIs were selected within 1.0 cm of the focal plane, within the transducer focal region (2–6 cm).

Errors in tissue speckle tracking have been categorized into two main types (Ramamurthy and Trahey, 1991). Jitter errors occur when the position of the actual correlation peak has been shifted inside of the main lobe due to noise. False peak errors occur when the position of the actual correlation peak has been shifted to one of the sidelobes. In tissue

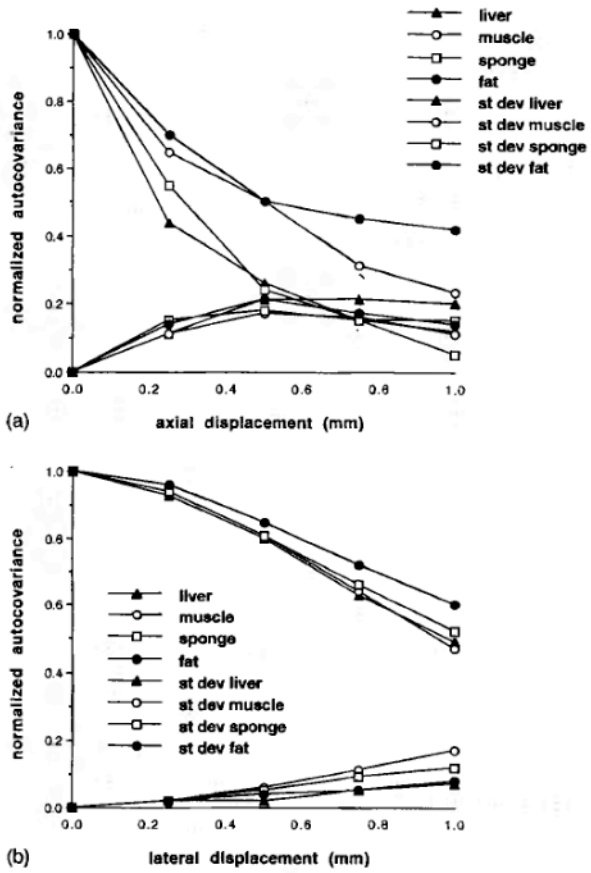

FIG. 3. Tissue autocovariance curves for (a) axial displacements and (b) lateral displacements. Each data point represents the average of five independent measurements and standard deviations are also graphed on each curve. Axial and lateral data lines were separated by at least two correlation lengths (4.0-mm axial separation and 16.0-mm lateral separation).

speckle tracking a correlation function can be generated and plotted from the correlation coefficients, at each position inside of the search area. The location of the correlation peak should correspond to the area of tissue providing the best match with the ROI and this location can be used to compute the displacement of the ROI. Correlation interpolation methods have been suggested to more precisely estimate the exact location of the true correlation peak, which may fall between data points (Jong *et al.*, 1991). Tissue tracking correlation functions will often have many of the same characteristics as the tissue autocorrelation curve. An autocorrelation curve with a broad main lobe will make it more difficult to locate the exact position of the peak correlation and will thus contribute to jitter errors (Chen *et al.*, 1994; Ramamurthy and Trahey, 1991; Wagner *et al.*, 1985). High amplitude sidelobes in the tissue autocorrelation curve will increase errors due to false peaks. Errors due to the classic peak hopping phenomenon can be reduced by using the moment, or center of mass, of the correlation function rather than simply the peak amplitude of the correlation function. The second-order statistics of speckle generated by different tissues should provide an indication of speckle tracking performance (Chen *et al.*, 1994; Ramamurthy and Trahey, 1991; Wagner *et al.*, 1985).

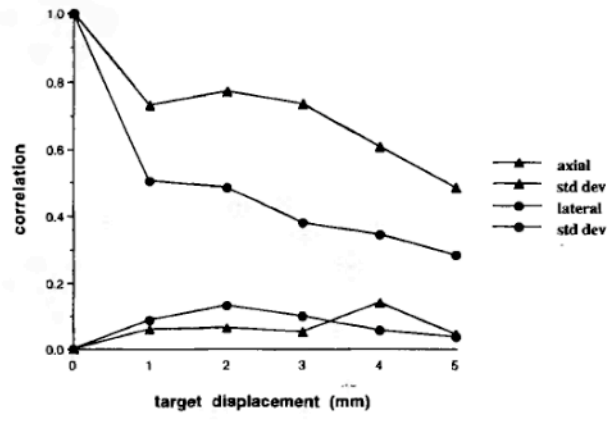

FIG. 4. Speckle pattern decorrelation in control sponge with translation. Each data point represents the average of five independent ROIs.

Covariance curves for all tissues were very similar and were within the 95% confidence intervals of one another. Based on the covariance curves, we would not expect speckle tracking performance to be significantly different in the various tissues in tracking over short distances. This was observed to be the case in both the axial and lateral directions for displacements up to 2.0 mm, where close to 100% and 80%, respectively, of all vectors were correctly tracked in all tissues. At larger displacements, particularly in the lateral direction, the difference in speckle tracking performance increases. For larger magnitude displacements (2.0–4.0 mm) the covariance curves may be less reliable predictors of tracking performance since the variance of autocovariance estimates was observed to increase significantly for larger lags. For all tissues, axial covariance curves were between 2 and 4 times narrower than the corresponding lateral covariance curves.

A major difficulty in estimating tissue covariance curves was the nonconstancy of received B-mode signal levels with increasing range. This problem was also observed by Wagner *et al.* (1985). To reduce this effect, autocovariances were computed only over axial regions where the received signals were relatively constant. However, the short sample intervals had the effect of increasing the variance of autocovariance curves. Results from averaging data from five different axial signals separated by at least two lateral correlation lengths (Wagner *et al.*, 1988) and taken from different images helped to reduce these variances.

Axial and lateral tissue autocovariance curves may be strongly affected by tissue anisotropies. Since muscle tissue contains a large number of myofibrils and other tissue microstructures which may result in periodic or highly correlated object structures (Wagner *et al.*, 1985), we might expect to see larger differences between muscle axial and lateral covariance curves than in liver, fat, and control sponge which more closely resemble isotropic media. However, we are less likely to see significant differences in the axial and lateral covariance curves if muscle fibers are randomly oriented, thus providing an equally random media in both directions. We would expect to see significant differences in axial and

lateral covariance curves if the majority of fibers were oriented in the same direction. For the muscle samples used in the study, muscle fiber orientation was observed to be largely random, with fibers neither parallel nor perpendicular to the ultrasound beam. We therefore did not observe more significant differences between muscle axial and lateral covariance curves relative to liver and fat tissue.

One of the problems encountered in assessing the performance of speckle tracking was whether to characterize tracking performance in terms of tracking error (geometric distance between actual and tracked displacement) or in terms of the percentage of correctly tracked vectors. Tracking errors provide more exact information about the magnitude of errors, yet are less useful in conveying the performance of tracking a large number of vectors. In addition, tracking errors for a single ROI can be misleading if the ROI happens to track very correctly or incorrectly. Performance measured in terms of the number of correctly tracked vectors has been used by previous groups (Trahey *et al.*, 1988). The drawback of this method is that no specific information is provided regarding the magnitude of errors for vectors that are correctly or incorrectly tracked. ROIs from different tissues may result in the same percentage of correctly tracked vectors for a given displacement. Yet the average magnitude of tracking errors may differ significantly. In fact, tracking errors between two different tissues may differ by as much as 30% for correctly tracked vectors. This difference could be even higher for incorrectly tracked vectors. In addition, the threshold of 30% (vectors tracked within 30% of actual displacement assumed correct) is somewhat arbitrary and the fact that search dimensions were selected to be 1.3× the actual displacement may positively bias results.

We have chosen to assess the performance of speckle tracking in terms of both tracking error and percentage of correctly tracked vectors. The latter is useful in conveying the performance of speckle tracking a large number of vectors, while the former provides more detailed information regarding the magnitude of tracking errors. All tracking errors were computed by averaging the errors from at least ten independent, nonoverlapping ROIs selected from within the focal region in all tissues. This provided additional insight into the true speckle tracking performance in each tissue. For example, in the axial dimension, while almost all vectors were correctly tracked in all tissues as defined by the 30% threshold, it is clear that the magnitude of tracking errors was largest in fat tissue. This could lead to larger errors in ultrasound displacement and strain imaging in fat compared to other tissues. Information about the magnitude of speckle tracking errors in each tissue would not be directly available from plots of the percentage of correctly vectors. Fat samples also produced the widest axial and lateral autocovariance curves compared to muscle, liver, and sponge which suggests a larger speckle cell size.

Tracking errors appeared to be consistently lower in muscle tissue relative to the control sponge, and consistently higher in fat for both axial and lateral translations. The improved tracking in muscle relative to liver and fat may be due to the presence of a large number of myofibrils, blood capillaries, and other muscle tissue microstructure, and the absence of such microstructure in liver and fat.

Tracking performance was observed to be substantially better in the axial direction for all tissues in terms of both magnitude of tracking errors and percentage of correctly tracked displacement vectors. Tracking performance also deteriorated for larger translations, results that are in agreement with previous studies (Chen *et al.*, 1994; Trahey *et al.*, 1986).

The accuracy of tissue speckle tracking relies heavily on the assumption that tissue samples produce speckle patterns that do not significantly change as the tissue is translated. The tracking of local tissue motion is valid only to the extent that the speckle patterns or landmarks being used remain constant. However, it is known that the speckle patterns in ultrasound images decorrelate or change as tissue translations are increased (Wagner *et al.*, 1985). Previous studies indicate speckle pattern decorrelation with translation to be generally independent of frequency (Trahey *et al.*, 1986). The magnitude of decorrelation for the fixed focus, mechanical scanner used in this study is shown in Fig. 4. Decorrelation of speckle patterns can result in significant errors in tissue speckle tracking (Akiyama *et al.*, 1988).

To minimize speckle pattern decorrelation, we have suggested an incremental tracking strategy (Chen *et al.*, 1994). Using this strategy, tissue regions are tracked incrementally over short distances. The incremental displacements can then be summed to compute a large net tissue displacement. Using this tracking strategy, tissue regions can be tracked over larger distances and the problem of speckle pattern decorrelation can be reduced.

As a specific example, suppose it is desired to track a particular tissue region on videotape data over a displacement on the order of 5.0 mm. It is known that tissue speckle patterns show signs of decorrelation for tissue displacements as small as 1.0 mm or less (Ramamurthy and Trahey, 1991). Instead of acquiring video frames of the tissue region before and after the 5.0-mm displacement (net tracking), where the tissue speckle patterns have already undergone significant decorrelation, a number of intermediate frames are acquired. The displacement of the tissue region can then be incrementally tracked over smaller displacements and summed to produce an estimate of the net displacement. Assuming three intermediate frames were acquired, then the incremental displacements might be on the order of 1.0 mm, effectively reducing tracking errors due to speckle pattern decorrelation. This approach assumes that acquiring intermediate data is feasible. We have found that this is normally the case when using video data since commercial frame-grabbing systems can digitize video data at a rate of 30 frames per second.

It should be understood that using incremental tracking, errors will accumulate with increasing displacement, independent of decorrelation effects. For example, for cases where there is very little or no decorrelation, net tracking will be more accurate. There is therefore a trade-off between incremental tracking step size and decorrelation effects.

Our results suggest that speckle tracking for ultrasound elasticity imaging in muscle and liver tissue should provide reasonably accurate results for small displacements (1.0–2.0 mm). For larger displacements, displacement estimates based

on direct speckle tracking may be less accurate, particularly in the lateral direction and in fat tissue. Use of an incremental tracking strategy should help reduce tracking errors due to speckle decorrelation.

V. CONCLUSION

The performance of tissue speckle tracking was investigated using porcine liver, muscle, fat, and sponge samples in calibrated tissue tracking measurements while keeping other speckle tracking parameters constant. Speckle tracking performance was characterized both in terms of the magnitude of tracking errors and in terms of the percentage of correctly tracked displacement vectors. Speckle tracking in muscle tissue, which contains a large number of myofibrils and other tissue microstructures, produced a higher percentage of correctly tracked vectors than other tissues. To minimize errors due to speckle decorrelation, an incremental tracking strategy was suggested. The use of an incremental tracking strategy may be particularly useful in ultrasonic strain imaging, where it may be necessary to track larger magnitude displacements or strains to achieve reasonable SNR (O'Donnell *et al.*, 1994).

Akiyama, I., Nakajima, N., and Yuta, S. (**1988**). "Movement analysis using b-mode images," Acoust. Imag. **17**, 499–505.

Chen, E., Hein, I., Adler, R., Carson, P., and O'Brien, W. (**1991**). "A comparison of the motion tracking of ultrasonic b-mode tissue images with a calibrated phantom," in *Proceedings of the IEEE Ultrasonics Symposium*, Orlando, FL (IEEE, New York), pp. 1211–1214.

Chen, E., Jenkins, W., and O'Brien, W. Jr. (**1994**). "The impact of various imaging parameters on ultrasonic displacement and velocity estimates," IEEE Trans. Ultrason. Ferroelectr. Frequency Control **41**, 293–301.

Chen, J., Jenkins, W., Hein, I. and O'Brien, W. D. Jr. (**1989**). "Design of a residue number system digital correlator for real-time processing in ultrasonic blood flow measurements," in *Proceedings of the IEEE International Symposium on Circuits and Systems* (IEEE, New York), pp. 208–211.

Goss, S., Johnston, R., and Dunn, F. (**1978**). "Comprehensive compilation of empirical ultrasonic properties of mammalian tissues," J. Acoust. Soc. Am. **64**, 423.

Goss, S., Johnston, R., and Dunn, F. (**1980**). "Comprehensive compilation of empirical ultrasonic properties of mammalian tissues II," J. Acoust. Soc. Am. **68**, 93–108.

Jong, P. D., Arts, T., Hoeks, A., and Renman, R. (**1991**). "Experimental evaluation of the correlation interpolation technique to measure regional tissue velocity," Ultrason. Imag. **13**, 145–161.

O'Donnell, M., and Engeler, W. E. (**1992**). "Correlation-based phase aberration correction in the presence of missing elements," IEEE Trans. Ultrason. Ferroelectr. Frequency Control **39**, 700–707.

O'Donnell, M., Skovoroda, A., Shapo, B., and Emelianov, S. (**1994**). "Internal displacement and strain imaging using ultrasound speckle tracking," IEEE Trans. Ultrason. Ferroelectr. Frequency Control **41**, 314–325.

Ramamurthy, B., and Trahey, G. (**1991**). "Potential and limitations of angle-independent flow detection algorithms using radio frequency and detected echo signals," Ultrason. Imag. **13**, 252–268.

Ryan, L., Lockwood, G., Bloomfield, T., and Foster, F. (**1993**). "Speckle tracking in high frequency ultrasound images with application to intravascular imaging," in *Proceedings of the IEEE Ultrasonics Symposium* (IEEE, New York), pp. 889–892.

Trahey, G., Hubbard, S., and von Ramm, O. (**1988**). "Angle independent ultrasonic blood flow detection by frame-to-frame correlation of b-mode images," Ultrasonics **26**, 271–276.

Trahey, G., Smith, S., and von Ramm, O. (**1986**). "Speckle pattern correlation with lateral aperture translation: Experimental results and implications for spatial compounding," IEEE Trans. Ultrason. Ferroelectr. Freq. Control **33**, 257–264.

Wagner, R., Insana, M., and Smith, S. (**1988**). "Fundamental correlation lengths of coherent speckle in medical ultrasonic images," IEEE Trans. Ultrason. Ferroelectr. Frequency Control **35**, 34–44.

Wagner, R., Smith, S., Sandrik, J., and Lopez, H. (**1985**). "Statistics of speckle in ultrasonic b-scans," IEEE Trans. Ultrason. Ferroelectr. Freq. Control **30**, 156–163.